Structural Transition in a Nematic LC Block Copolymer Induced by the Transition to the LC Phase

J. Sänger,[†] W. Gronski,*[,†] S. Maas,[†] B. Stühn,*[,‡] and B. Heck[‡]

Institut für Makromolekulare Chemie and Fakultät für Physik, Universität Freiburg, D-79104 Freiburg, Germany

Received April 15, 1997; Revised Manuscript Received August 12, 1997[⊗]

ABSTRACT: The morphology of a liquid-crystalline ABA triblock copolymer with polystyrene (PS) blocks (12 vol %) and a side chain nematic liquid crystalline B block has been studied by TEM and temperature dependent SAXS measurements. Above the clearing temperature (T_c = 122 °C) the morphology is characterized by a body-centered cubic (bcc) lattice of polystyrene spheres. The transition to the nematic phase induces a reversible transition to a morphology of hexagonally packed cylinders by coalescence of the PS spheres along the [1,1,1] direction of the bcc lattice.

Introduction

The synthesis of hybrid LC/I block copolymers consisting of liquid-crystalline (LC) and isotropic (I) blocks has opened the possibility of studying fundamental problems of the interdependence of liquid crystalline order and microdomain morphology. An overview of the present state of research has been given in recent reviews.[1,2] One of the questions is which symmetries of the liquid-crystalline phase coexist with the various symmetries of regular microdomain morphologies that are known for isotropic block copolymers. Though various synthetic procedures have been described, little is known on the phase behavior of these systems. Up to now the only systematic study has been carried out on polystyrene/poly[2-(3-cholesteryloxycarbonyloxy)-ethyl methacrylate] (PS/PChEMA) block copolymers in which the corresponding LC homopolymer has a smectic A phase.[3,4] In this system the sequence of microdomain morphologies that is generally observed for isotropic block copolymers is modified and the LC phase proved to be dependent on the LC microdomain geometry. Because of the chemical instability of the block copolymer above the clearing temperature (200 °C) the microdomain morphology could not be studied in the isotropic state. Therefore the question remains open whether the transition from the isotropic to the liquid-crystalline state can induce a morphology change. An effect can be expected to exist in a system in which the symmetry of the microdomains is incommensurate with the symmetry of the liquid-crystalline phase. In this case the elastic energy of director distortions may force the microdomains to an energetically more favorable arrangement. Led by these ideas, we investigate in this paper the effect of the isotropic−nematic phase transition in a block copolymer in which spherical microdomains are embedded in a continuous LC phase forming matrix.

Experimental Section

Material and Sample Preparation. The LC/I block copolymer studied is an ABA triblock copolymer with polystyrene A-blocks and a liquid-crystalline side-chain center block with the structure shown in Chart 1. The block copolymer was synthesized by hydroboration of the poly(1,2-butadiene) center block of a corresponding precursor triblock copolymer

Chart 1

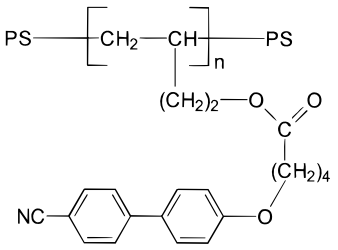

prepared by anionic polymerization and subsequent introduction of the mesogens by esterification of the hydroxyl groups.[5] The synthesis of the mesogen and details of the specific preparation and characterization of the triblock copolymers **1** are published elsewhere.[6] The LC phase behavior of the block copolymers is dependent on the number x of methylene groups of the spacer. In this work a nematic system with $x = 4$ is investigated. The LC phase behavior is characterized by the sequence g/34/n/122/i.[6] The styrene content is 12 wt %, and the total molecular weight is 84 000, as calculated on the basis of the the molar mass of the precursor block copolymer and 100% conversion. The block copolymer proved to be thermally stable after annealing for 48 h at 180 °C under argon. For morphological studies by TEM and SAXS measurements, block copolymer specimens obtained by evaporation from a solution in tetrahydofuran were spin casted from $CHCl_3$. After drying under vacuum at 80 °C, the samples were heated to 160 °C above the clearing temperature of the LC phase and annealed at this temperature under argon for 8 h. From this temperature the samples were slowly cooled over 12 h to room temperature (RT). For quenching from elevated temperatures these samples were annealed for 45 min at the specified temperature and frozen in liquid nitrogen.

Small Angle X-ray Measurements. The small angle X-ray scattering experiments (SAXS) were performed in a Kratky compact camera (PAAR, Graz, Austria). The Cu Kα radiation from a sealed X-ray tube is reflected from a graphite monochromator. The resulting wavelength is $\lambda = 0.154$ nm. The accessible range of scattering vectors $q = (4\pi/\lambda) \sin \theta$ is $0.1 < q/\mathrm{nm}^{-1} < 3$. 2θ is the scattering angle. The scattered intensity is recorded with a scintillation counter in a step scanning mode. The sample is contained in a brass sample holder with acetate windows. The holder together with the collimation system is seated in an evacuated chamber. The temperature of the sample holder is measured with a platinum resistor (Pt100) and its stability is better than 0.2°. Data collection and temperature regulation are controlled with a computer. The background is corrected by subtraction of the scattering from an empty sample holder. The intensity is normalized to the incoming flux with the help of the moving slit device (PAAR, Graz, Austria). The effect of the slitlike cross section of the beam is accounted for by desmearing the data using standard procedures[7] to result in the scattering cross section in units of the Thomson cross section σ_{Th}.

* To whom correspondence should be addressed.
† Institut für Makromolekulare Chemie.
‡ Fakultät für Physik.
⊗ Abstract published in *Advance ACS Abstracts,* October 1, 1997.

S0024-9297(97)00518-4 CCC: $14.00

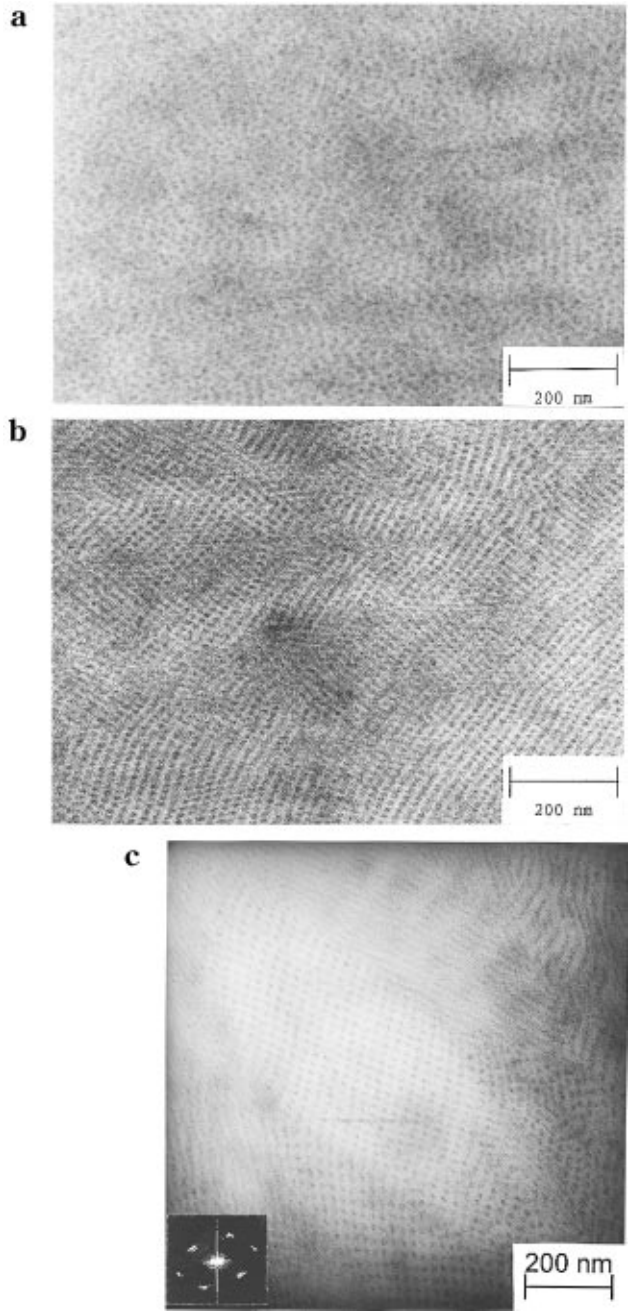

Figure 1. TEM micrographs of block copolymer samples (a) quenched from 200 °C, (b) quenched from 150 °C, and (c) slowly cooled from 160 °C to RT.

Results

Transmission Electron Microscopy. In Figure 1a−c are displayed TEM micrographs of specimens subjected to different temperature treatments. The polystyrene domains appear dark due to staining with RuO_4. First the samples were annealed in the isotropic state in order to establish the equilibrium morphology. Then they were cooled at different cooling rates from various annealing temperatures in order to see whether the isotropic equilibrium morphology is affected by the isotropic/nematic transition. After annealing at 200 °C and quenching, the morphology of the spherical PS domains is that expected for the composition of the block copolymer (Figure 1a). After annealing at 150 °C and quenching, the spherical morphology is still present (Figure 1b). The micrograph of Figure 1c was obtained after slow cooling from the melt at 160 °C. The micrograph should therefore be representative of the equilibrium morphology in the nematic phase. In the lower left and lower center part of the micrograph and on the right side we see now rods in different orientations. In the middle a slightly deformed hexagonal arrangement of circular areas is apparent, which is typical for hexagonally packed cylinders cut perpendicular to the cylinder axis. The inset represents a Fourier transformation of the section containing preferentially the hexagonal structures.

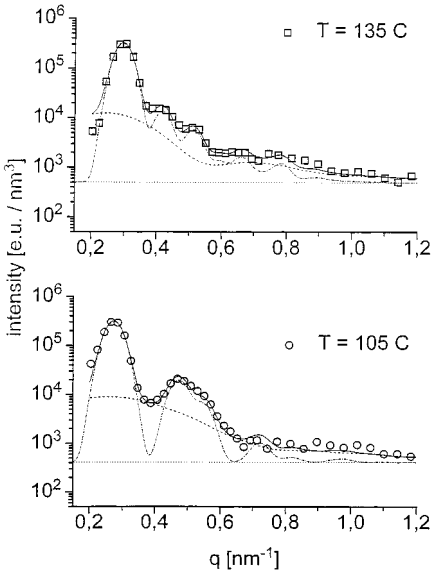

Figure 2. SAXS profiles at 105 and 135 °C that are typical for the low- and high-temperature phases of the block copolymer. Statistical errors are of the size of the symbol. The full line corresponds to a fit of eq 1 using the hpc model for the low-temperature phase and the bcc model for the high-temperature phase. The broken lines are the components of I according to eq 1.

Small Angle X-ray Measurements. The pictures obtained with electron microscopy suggest a spherical domain morphology at high temperatures in the isotropic phase and cylindrical domains in the nematic phase. It is, however, difficult to assign a well-defined temperature to these measurements, as the sample has to be cooled or quenched to a low temperature in order to prepare the necessary thin slides for the electron microscope. It is therefore desirable to determine the mesostructure of this system in dependence on temperature with SAXS. These measurements were performed in heating and cooling runs in steps of 5 or 10 deg. Data collection at each temperature takes about 20 min, and the sample was annealed for another 30 min after each temperature change. In Figure 2 we display the results obtained at 105 and 135 °C, respectively. The temperatures chosen are above and below the transition between the liquid-crystalline phases of the continuous matrix. The scattering vector regime of the SAXS profiles, however, refers to distances in direct space between 4 and 70 nm. The drastic change of the profile between both states is therefore related to a change of the mesostructure. In the following we analyze the scattering profiles in order to characterize the structural change of the mesostructure. It has been shown previously that such an analysis may be used to obtain the lattice parameters as well as the domain sizes for spherical domains on a body-centered cubic (bcc) lattice[8,9] and cylindrical domains in hexagonal packing (hpc).[10] We treat the sample as an arrangement of crystalline grains with no preferred orientation. It is therefore analogous to a polycrystalline powder. The

scattered intensity is in general the sum of three components:

$$I(q) = I_{\text{Bragg}} + I_{\text{diff}} + I_{\kappa} \tag{1}$$

The finite compressibility of the material gives rise to density fluctuations that are seen in the scattering profile as a q independent background I_{κ}. The most prominent features of the profile are several maxima that are the result of the Bragg reflections from the macrocrystalline lattice formed by the PS domains. Their contribution to the intensity is denoted I_{Bragg}. Quite generally, the intensity of each peak is the product of the form factor of the scattering particle $\Phi^2(q_{\text{hkl}})$ and the multiplicity of the reflection j_{hkl}:

$$I_{\text{Bragg}}(q) = \sum_{\{\text{hkl}\}} \overline{\Phi^2}(q_{\text{hkl}}) \frac{j_{\text{hkl}}}{q^2} G_{\text{hkl}}(q;\sigma) \exp\{-{q_{\text{hkl}}}^2 u^2/3\} \tag{2}$$

Equation 2 contains a Lorentz factor $1/q^2$ for an isotropic distribution of grains. $G_{\text{hkl}}(q;\sigma)$ denotes a normalized Gaussian centered at q_{hkl} with a variance σ. The bar denotes an average over the size distribution of the microdomains. The peak position q_{hkl} is directly related to the lattice constant. As a result of the large size of the microdomains, the intensity of the Bragg reflections is modulated by the form factor $\Phi(q)$. Its explicit form for spheres[8] or cylinders[10,11] is inserted into eq 2. The average over the size distribution is formulated as an integral over a Gaussian distribution of radii and performed numerically in the fit procedure.

The third term in eq 1 arises from the positional disorder and the size distribution of the microdomains. We approximate it as

$$I_{\text{diff}} \propto (1 - \exp(q^2u^2/3))\overline{\Phi}^2 + (\overline{\Phi^2} - \overline{\Phi}^2) \tag{3}$$

u^2 is the mean square displacement of the microdomain from its lattice position.

The comparison of the profiles in Figure 2a,b shows different peak positions and a distinct change in their relative intensities. The structure at 135 °C is in accordance with the assumption of spherical domains on a bcc lattice, whereas the lower temperature profiles correspond to hexagonally packed cylindrical microdomains. Equation 1 is used to fit the data and to obtain the lattice constants and the size of the microdomains at each T.

The result of this fit procedure is included in Figure 2 as the full line. Also shown in the figure are the three components according to eq 1. At 135 °C we use the model of spherical domains on a bcc lattice. At 105 °C a good description of the data is only obtained within the hpc model. The Gaussian width of the Bragg reflections turns out to be $\sigma = 0.06$ nm^{-1} independent of T. The size distribution of the sphere radii R_{sph} is rather narrow with a variance $\sigma = 1.3$ nm. For the cylindrical domains we determine R_{cyl} with $\sigma = 1.0$ nm for the radius. The height of the cylinders cannot be reliably obtained, as it would only be contained in the diffuse scattering contribution.

The transition between both structures occurs discontinuously at $T_c = 124(\pm 5)$ °C. Figure 3 shows the position q^* of the dominant peak in the scattering pattern with dependence on temperature. At high temperatures, in the bcc state, q^* is the {110} group of reflections and the distance between neighboring spheres

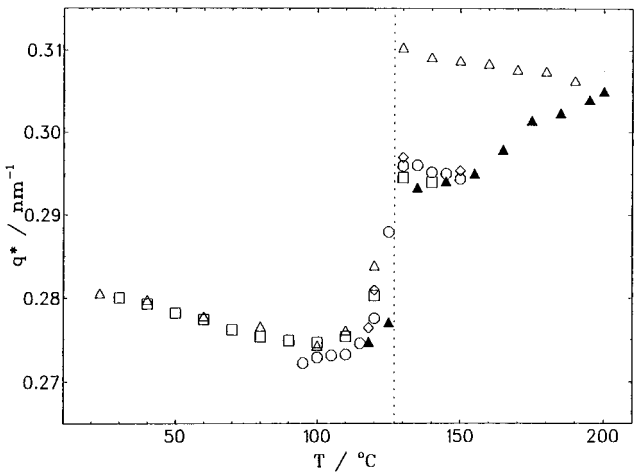

Figure 3. Position of the maximum of the SAXS structure factor. Heating (filled symbols) and cooling (open symbols) runs are shown. Different symbols refer to repeated measurements. The perpendicular line marks the transition temperature.

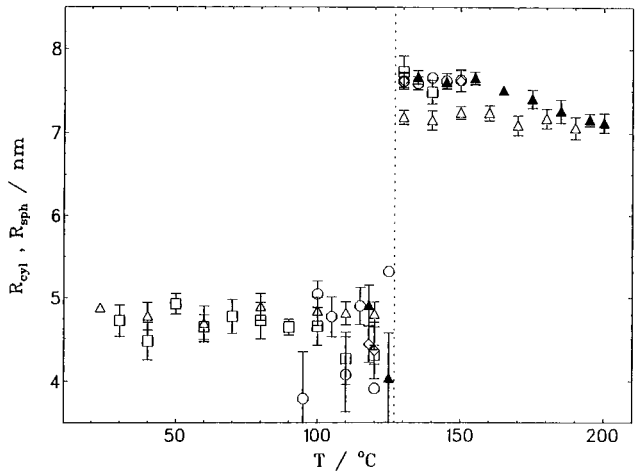

Figure 4. Size of the PS microdomains measured by the R_{sph} above T_c and R_{cyl} below: heating (filled symbols); cooling (open symbols). Different symbols refer to repeated measurements.

a_{sph} is $a_{\text{sph}} = 2\pi\sqrt{2}/q^*$. Below T_c we have $a_{\text{cyl}} = (4\pi/\sqrt{3})/q^*$ with a_{cyl} being the distance between two cylindrical domains. The position of q^* varies weakly with T above and below T_c but shows a discontinuity of 7% at the phase transition. Figure 3 includes data from heating (filled symbols) and cooling (open symbols) runs. Whereas below T_c we find a superposition of both sets, there is a clear difference observable between both sets above 160 °C. A transition into a metastable state appears to occur at that temperature, which does not significantly change the shape of the diffraction pattern.

A further result of the analysis of the SAXS pattern according to eq 1 is the size of the PS domain. Above T_c this is the average radius of the sphere R_{sph}, below the radius of the cylinder R_{cyl}. In Figure 4 we show the result for both quantities again for heating and cooling cycles. The cylinders do not change their cross section with variation of T. At high temperatures, however, we find a decrease in the size of the spherical domains that is not compensated for when the sample is cooled back to the transition temperature. The same temperature dependence is found for the lattice constant a, as shown in Figure 5.

In both states we can calculate the volume fraction f of the PS domains from the structural parameters. f must be consistent with the chemical composition of our

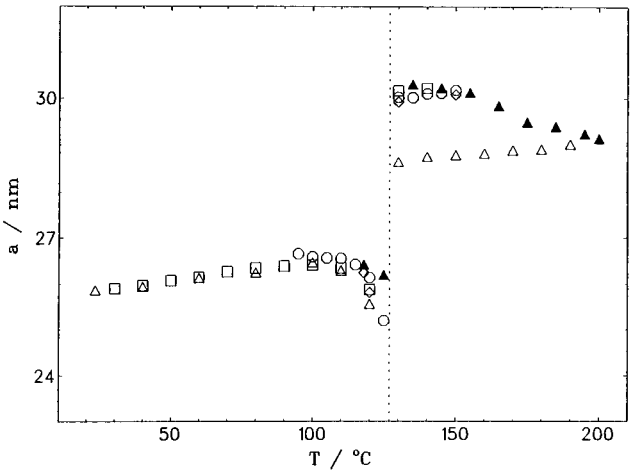

Figure 5. Lattice constant *a* for both states: heating (filled symbols); cooling (open symbols). Different symbols refer to repeated measurements. The temperature dependence of *a* follows that of the domain size (Figure 3).

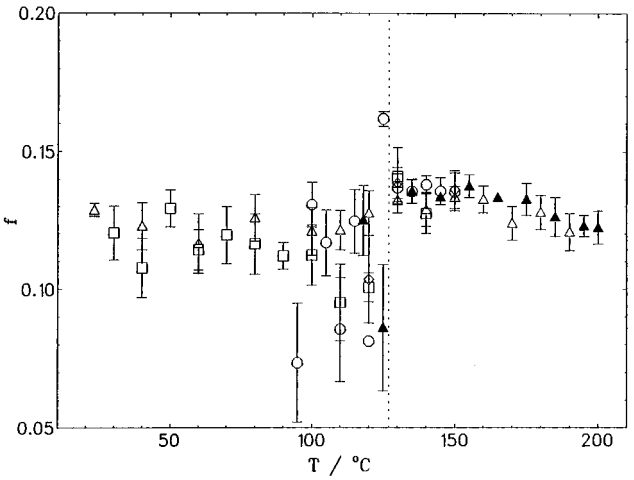

Figure 6. Calculated volume fraction of the PS domains. It remains constant through the transition and is in accordance with the chemical composition of the block copolymer. Symbols are as in Figures 3−5.

block copolymer. In Figure 6 we compare the calculated value from the SAXS measurements with the chemical composition. The agreement is good within experimental error. The system therefore appears to be fully microphase separated. The larger scatter near and the small jump at the phase transition is probably caused by the imperfection of the model not describing the detailed nature of the transition state between the two morphologies.

Discussion

The transition from the bcc morphology of PS spheres to the hpc morphology of PS cylinders, which is induced by the isotropic/nematic transition of the continuous matrix, can be understood if one considers the constraints on the director distribution exerted by the inner boundaries of the system. It has been shown that spherical particles suspended in a nematic liquid-crystalline matrix introduce complex distortions of the director field in the vicinity of the particle surfaces.[12] The elastic forces generated by these distortions lead to interactions between the particles, which can be repulsive or attractive depending on the boundary conditions. For strong radial (homeotropic) anchoring of the mesogens on the surface the particles are repelled

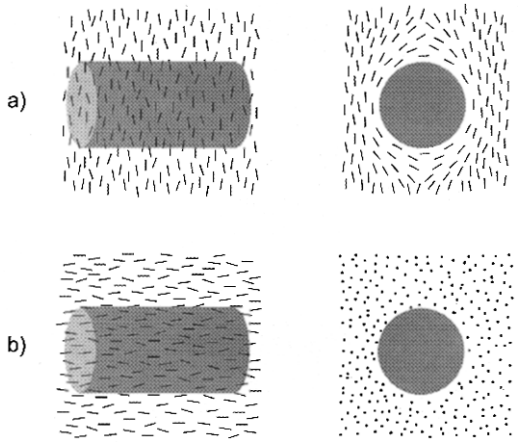

Figure 7. Two cases of mesogen orientation in the nematic phase with respect to the orientation of the PS cylinders. The ratio of the cylinder radius and of the mesogen length in the picture describes the realistic size ratio for the system.

from each other; for soft homoeotropic anchoring the particles are attracted at close distances. For the case of the nematic block copolymer considered here, the mesogens are probably oriented planar to the surface. This can be derived from the fact that the polymer chains are preferentially oriented perpendicular to the surface[13] and the mesogens of the LC homopolymer orient pependicular to the stretching direction.[6] The first result was proven by neutron scattering studies on conventional block copolymers of lamellar morphology[13]; the second information comes from WAXS measurements[6] on a stretched specimen of the nematic block copolymer of this study. For planar boundary conditions the director field about a single sphere causes a bipolar configuration that minimizes the elastic energy and results in a distortion of the PS spheres, as observed in TEM images.[3]

The interaction of spherical particles with homogeneous boundary conditions has not been treated theoretically and it is not known how the distortions of the director field interact with the three-dimensionally ordered bcc lattice. However, the experimental evidence suggests that there are similar attractive forces between the particles as in the case of weak homeotropic anchoring. As a consequence a coalescence of the spheres to rods can be imagined. The process probably proceeds via a deformation of the spheres that has been observed experimentally. The transformation of the spherical to a cylindrical morphology minimizes the elastic energy because the rods have the same symmetry as the undisturbed director field. There are two relative orientations that minimize the elastic energy: in one situation the director is directed perpendicular to the cylinder axis (Figure 7a), in the other the cylinder axis is parallel to the director (Figure 7b). In both cases the mesogens are essentially oriented parallel to the cylinder surface and the polymer chains have the least packing energy at the interface. The first situation has been observed in PS/PChEMA block copolymers with PS cylinders in a continuous smectic phase.[2,3] The second case has been recently observed in dilute solutions of LC/I diblock copolymers in nematic solvents.[1,14] Block copolymers with a high fraction of the nematic block form threadlike structures that are perfectly ordered with their long axis parallel to the director of the nematic solvent and the mesogens are oriented parallel to the interface.

In the bulk state of a block copolymer with isotropic spheres on a bcc lattice the situation is more compli-

cated. In the isotropic state at the given composition the spherical morphology minimizes the free energy arising from essentially two contributions: the contact enthalpy in the narrow interfaces between the microdomains and the entropy loss associated with extended chain configurations to ensure homogeneous density.[15] In the nematic phase the total free energy additionally includes the elastic free energy of the nematic phase. While the spherical morpholgy minimizes the total free energy in the isotropic state this morphology does not conform with the minimum energy in the nematic phase due to the high penalty for the elastic energy. The morphology having the next higher free energy in the isotropic state is the hpc cylindrical morphology. During the transition to the nematic state the structural transition bcc → hpc occurs because the higher energy of the hpc phase in the isotropic state is more than compensated for by the loss of the elastic free energy. A lowering of the elastic free energy would also be reached by a transition to a morphology with planar surfaces, i.e., a lamellar morphology. However, the higher segmental volume of the LC block favors the formation of domains with a convex surface.

In a bcc lattice a transition to a cylindrical morphology through coalescence of spheres is possible in two ways. Either this process can take place along the [100], [010], and [001] directions of the crystallographic axes or in the directions along the diagonal of the elementary cell, i.e., in the [1,1,1] direction. The first possibility leads to a tetragonal cylindrical structure as observed for PS cylinders of the smectic PS/PChEMA block copolymer.[16] Our SAXS measurements clearly show the presence of a hexagonal structure in the nematic phase. The structure can be realized by a merging of the PS spheres along the [1,1,1] direction. If this mechanism is taking place, the lattice constant of the hpc lattice must be identical with the smallest distance between the spheres in the bcc lattice $(a/2)\sqrt{3} = 0.866a$ where a is the lattice constant of the bcc lattice. This is the case, as can be verified by comparison of the lattice constants in Figure 5.

Besides the favorable packing of the polymer, there is another reason why the coalescence of the spheres occurs along the [1,1,1] direction. It is along this direction where the distance between the spheres is minimal, i.e., the transition is possible with the least deformation of the PS domains. That the spheres are stretched along the [1,1,1] direction is evident in Figure 4. The radii of the cylinders are about two-thirds of the radii of the spheres. The deformation of the non-liquid-crystalline domains is essential for the transition to occur in the bulk to avoid the building up of stresses. During the transition, a rearrangement of the polymer chains must take place. As the spheres are stretched along the [1,1,1] direction, the block junctions on the surface are forced to migrate from the poles to the equator; i.e., the chains rotate toward the $[\bar{1},1,1]$ direction vertical to the cylinder axes. During this process the bridging chains between neighboring merging spheres will be transformed to loops during the transition. The generation of loops is typical for a triblock copolymer, as in the present study. It is likely that the deformation of the isotropic microdomains and the motion of the chains within the microdomains are an essential condition for the structural transformation. This requires that the glass transtion temperature of the isotropic block is sufficiently smaller than the clearing temperature, which is fulfilled for the system investigated.

A characteristic feature of the transition is its reversibilty. When the nematic phase is entered, the elastic energy of the director field enforces the transition bcc → hpc. Upon entering the isotropic phase, the director field disappears and the transition is driven in the reverse direction because the cylindrical morphology is unstable in the isotropic phase. The sharpness of the transition reflects the high driving force due to the first order nematic/isotropic transition in both directions. The analysis of the SAXS intensity distribution above and below T_c does not give evidence of the coexistence of spherical and cylindrical morphologies; i.e., the transformation is complete within the time scale of the heating and cooling scans. While the transition to the nematic phase appears to create a cylindrical morpholgy in an equilibrium state, the equilibrium spherical morpholgy is not established immediately when entering the isotropic phase. Upon heating, the radius of the PS spheres (Figure 4) and the constant of the bcc lattice (Figure 5) first remain constant up to $T \approx 160$ °C. Between 160 and 180 °C these parameters decrease by about 4% and 7%, respectively. Above 180 °C the equilibrium has been approximately reached, as shown by the approximate constancy of the structure parameters during the subsequent cooling.

Outlook

It is well-known that thin nematic films can be oriented by shear, leading to a uniaxial director orientation, which is the basis for LC display devices. Likewise, it is known that macroscopic single crystals are formed when isotropic block copolymers with cylindrical morphology are oriented by planar shear[17] or by extrusion.[18] If a nematic block copolymer film with cylindrical microdomains is subjected to shear, a single crystal may be generated in which the director and the cylinders are oriented parallel or vertical to each other, as depicted in Figure 7. Orientation experiments on the block copolymer will be described in a forthcoming paper.

Acknowledgment. The work was supported by the "Sonderforschungsbereich 428" of the "Deutsche Forschungsgemeinschaft".

References and Notes

(1) Walther, W.; Finkelmann, H. *Prog. Polym. Sci.* **1996**, *21*, 951.
(2) Fischer, H.; Poser, S. *Acta Polym.* **1996**, *47*, 413.
(3) Fischer, H.; Poser, M.; Arnold, M. *Liq. Cryst.* **1995**, *18*, 503.
(4) Fischer, M.; Poser, S.; Frank, W.; Arnold, M. *Macromolecules* **1995**, *28*, 6957.
(5) Adams, J.; Gronski, W. *Makromol. Chem., Rapid Commun.* **1989**, *10*, 553.
(6) Sänger, J.; Gronski, W. *Macromol. Chem. Phys.*, submitted for publication.
(7) Strobl, G. *Acta Crystallogr.* **1970**, *A26*, 367.
(8) Schwab, M.; Stühn, B. *Phys. Rev. Lett.* **1996**, *76* (6), 924.
(9) Schwab, M.; Stühn, B. *Colloid Polym. Sci.* **1997**, *275*, 341.
(10) Heck, B.; et al. *Macromolecules*, submitted for publication.
(11) Mittelbach, P.; Porod, G. *Acta Phys. Aust.* **1961**, *14*, 405.
(12) Terentjev, E. M. *Phys. Rev. E* **1995**, *51*, 1330.
(13) Matsushita, Y.; Nakao, Y.; Saguchi, R.; Mori, K.; Choshi, H. *Macromolecules* **1988**, *21*, 1802.
(14) Walther, M.; Bohnert, S.; Derow, S.; Finkelmann, H. *Macromol. Rapid Commun.* **1995**, *16*, 621.
(15) Helfand, E.; Wassermann, Z. R. *Macromolecules* **1976**, *9*, 879.
(16) Fischer, H. *Polym. Commun.* **1994**, *35*, 3786.
(17) Hadziioannou, G.; Mathis, A.; Skoulios A. *Colloid Polym. Sci.* **1979**, *257*, 136.
(18) Keller, A.; Olugosz, J.; Folkes, M. J.; Pedemonnte, E.; Scalise, F. P.; Willmonth, F. J. *J. Phys.* **1971**, *32*, C5a, 295.

MA970518W